Available online at www.sciencedirect.com
SCIENCE DIRECT®
Geoderma xx (2005) xxx–xxx
GEODERMA
www.elsevier.com/locate/geoderma

Spatial patterns of soil organic carbon on hillslopes: Integrating geomorphic processes and the biological C cycle

Kyungsoo Yoo[a,*], Ronald Amundson[a], Arjun M. Heimsath[b], William E. Dietrich[c]

[a]*Division of Ecosystem Sciences, University of California, Berkeley, CA 94720-3110, USA*
[b]*Department of Earth Sciences, Dartmouth College, Hanover, NH 08755, USA*
[c]*Department of Earth and Planetary Science, University of California, Berkeley, CA 94720, USA*

Received 30 March 2004; received in revised form 29 October 2004; accepted 12 January 2005

Abstract

Significant portions of the global soil organic carbon (SOC) pool must reside on sloping terrains where the spatial distribution of SOC reflects the combined effects of geomorphic processes and biological C cycling. Using a newly developed soil C mass balance model that explicitly includes soil production and sediment transport, we investigated the relative roles of sediment production/transport vs. biological C cycling in creating the observed spatial patterns of SOC storage within two grass-covered hillslopes in California. The study sites differed in bedrock geology, climate, and erosion rates. Measurements of SOC, soil texture, plant C inputs, and soil thickness were combined with topographic surveys and published soil erosion and production rates in the analysis. Soil thickness was found to be the key control on SOC storage, and soil thickness is balance between soil production and curvature-dependent erosional losses. Additionally, topographically varying rates of plant C inputs, decomposition rates, and SOC erosional losses or depositional inputs were found to only partially explain the observed SOC storage patterns. We used the measured relationships between SOC storage, soil thickness, and topographic curvature to create SOC storage maps of the two watersheds. At both sites, about 70% of the hillslope SOC is stored in depositional areas that are susceptible to episodic mass wasting. At the drier site, there was a larger SOC storage despite the lower soil C % because the clay-rich bedrock resulted in the development of relatively thick soils for a given slope curvature. We conclude that the geomorphic processes driving soil thickness provide fundamental mechanisms that control the spatial SOC patterns on vegetated hillslopes.

Keywords: Soil organic carbon; Soil erosion; Soil production; Sediment transport; Hillslope

1. Introduction

For more than six decades, it has been recognized that the spatial pattern of soil organic carbon (SOC) is controlled by a combination of environmental or state

* Corresponding author. Tel.: +1 510 643 6910; fax: +1 510 642 6632.
E-mail addresses: kyoo@nature.berkeley.edu (K. Yoo), earthy@nature.berkeley.edu (R. Amundson), Arjun.Heimsath@Dartmouth.EDU (A.M. Heimsath), bill@geomorph.berkeley.edu (W.E. Dietrich).

0016-7061/$ - see front matter © 2005 Elsevier B.V. All rights reserved.
doi:10.1016/j.geoderma.2005.01.008

factors (Jenny, 1941), with one of the more commonly studied being topography. On a global scale, where climatic variations exert a first order control on the amounts (Jenny, 1928; Post et al., 1982) and cycling rates (Sanderman et al., 2003; Trumbore et al., 1996) of soil C, topography exerts a strong secondary control within a given region.

Most research on topographic controls on SOC has focused on hillslopes (Aandahl, 1948; Brejda et al., 2001; Burke et al., 1999; Garten and Ashwood, 2002; Honeycutt et al., 1990; Hook and Burke, 2000; Kleiss, 1970; Schimel et al., 1985; Yonker et al., 1988; Young and Hammer, 2000). In these studies, observed SOC variations have been attributed to topographic variations of plant inputs, decomposition, soil texture, nutrients, water, and/or soil C erosion and deposition. While a strong linkage between SOC and geomorphic processes has been recognized (notably in Schimel et al., 1985), there has been no way to quantitatively examine these effects on a meter by meter basis for an entire hillslope. Recently, researchers used digital elevation models (DEM) to statistically link soil properties to the topographic attributes such as wetness index, slope gradient, and curvature (e.g., Gessler et al., 2000; Moore et al., 1993). These studies, while informative, are not based on fundamental physical models and thus questions remain about the broad applicability of one hillslope attribute or another to a regional or global scale. Recently, linkages between sediment transport processes to various soil properties were undertaken (e.g., Minasny and McBratney, 1999, 2001; Park et al., 2001; Rosenbloom et al., 2001), but a process-based understanding of topographic controls on SOC, in general, has not been fully explored.

In this study, we examine the mechanisms creating the spatial distribution of SOC storage within two Coastal California hillslopes where previous geomorphic works revealed the processes and rates of soil erosion and production (Heimsath et al., 1997; McKean et al., 1993). Besides topography, other soil forming factors such as climate, geology, and vegetation are approximately invariant within each hillslope. We develop a new soil C mass balance model that explicitly includes not only biological C fluxes, but also C erosion and soil thickness as controlled by soil erosion and production. Guided with this conceptual framework, we examine the degree that geomorphic processes of soil production and erosion, independent of biological C cycling, affect the spatial pattern of hillslope SOC. This paper is a companion to Yoo et al. (in press), which focuses on quantifying SOC erosion rates and temporal variations of SOC storages in the same watersheds.

2. Background and development of theory

Most SOC mass balance models assume that changes in SOC storage (within a predetermined soil depth) occur through changes in net primary productivity (NPP) or decomposition:

$$\frac{dS}{dt} = \underbrace{I}_{\text{plant inputs}} - \underbrace{kS}_{\text{decomposition}} \quad (1)$$

where S=SOC storage [ML^{-2}], I=NPP [$ML^{-2}T^{-1}$], and k=decomposition rate constant [T^{-1}]. By using this model at regional to global scales, climate has been shown to be an important determinant of SOC storage (for a review of this subject see Amundson, 2001).

Recently, Stallard (1998) suggested that accelerated soil erosion and deposition in agricultural watersheds could be an unrecognized C flux in the global C budget, which can be described as:

$$\frac{dS}{dt} = \underbrace{I}_{\text{plant inputs}} - \underbrace{kS}_{\text{decomposition}} - \underbrace{\rho_\varepsilon C_\varepsilon E}_{\text{erosion}} \quad (2)$$

where E=soil erosion rate (deposition if negative) [LT^{-1}], ρ_ε=bulk density of eroding soils [ML^{-3}], and C_ε=mass fraction of C in eroding soils [MM^{-1}].

The mass balance models described above do not explicitly consider soil thickness. While soil thickness sets the boundary condition for SOC storage, SOC storage has been generally reported for a predetermined soil depth interval, ignoring the spatial and temporal variation in soil thickness. To evaluate the role of soil thickness, we incorporated into the SOC mass balance model a soil production-erosion sub model, where soil thickness is viewed as the balance between these two processes (Fig. 1):

$$\frac{dS}{dt} = \int_0^H \left[\underbrace{\frac{I_z}{\Delta z}}_{\text{plant input}} - \underbrace{k_z \rho_z C_z}_{\text{decomposition}} \right] dz - \underbrace{\rho_\varepsilon C_\varepsilon E}_{\text{erosion}} \quad (3)$$

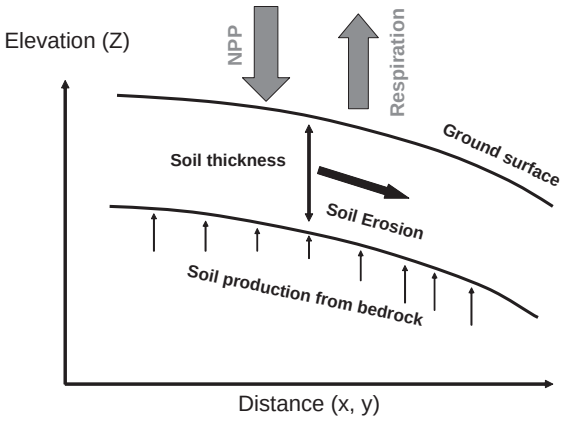

Fig. 1. A schematic diagram of processes affecting hillslope soil thickness and SOC. Downslope sediment transport (erosion) is driven by physical and biological mixing processes, and as a result, the entire soil mantle is transported downslope. Modified from Heimsath et al. (1997).

where

$$\frac{\partial H}{\partial t} = \underbrace{P}_{\text{soil production}} - \underbrace{E}_{\text{erosion}} \tag{4}$$

where z=soil horizon depth relative to the ground surface [L], H=vertical soil thickness [L], and P=soil production rate [LT^{-1}]. Soil is defined as transportable material derived from saprolite that retains bedrock fabric. The SOC storage at a given topographic location in this model is now a function of biological C cycling, C erosional loss or deposition, and soil thickness determined by soil erosion and production.

While our soil C mass balance models (Eqs. (3) and (4)) are valid regardless of the erosion process, we apply the model here to soil-mantled hillslopes where erosion by overland flow is rare. In these environments, soil transport occurs by biological activity (e.g. animal burrowing or root decay) and/or abiotic processes (e.g. rain splash or swelling and shrinking of clay soils), whose rates are "slope-dependent" (Culling, 1963; Gilbert, 1909). The net erosion rate (E) [LT^{-1}] is the difference between the inputs and outputs of the slope-dependent sediment flux, and is thus curvature dependent:

$$E = K\left(-\nabla^2 Z\right) \tag{5}$$

where K=diffusivity [L^2T^{-1}] and $-\nabla^2 Z$=the negative curvature of the ground surface (convex when positive) [L^{-1}]. We assume a constant diffusivity within a hillslope. In the face of erosion, a soil mantle persists due to soil production from bedrock. We focus on hillslopes where bedrock converts to soil by physical disruption, the rate of which decreases exponentially with increasing soil thickness (Heimsath et al., 1997, 2000, 2001a,b):

$$P = \frac{\rho_r}{\rho_s}\varphi_0 e^{-H/\alpha} \tag{6}$$

where φ_o=the soil production rate of exposed bedrock [LT^{-1}], α=the depth where the soil production rate decreases to the 1/e of φ_o [L].

Given sufficient time, a steady state soil thickness (when Eq. (4)=0) may develop on convex slopes:

$$H = \ln\left[\frac{\rho_r}{\rho_s}\frac{\varphi_o}{K\left(-\nabla^2 Z\right)}\right]^{\alpha} \tag{7}$$

This steady state soil thickness varies inversely with increasing convexity (Dietrich et al., 1995; Heimsath et al., 1997).

On concave hillslopes soils thicken due to sediment input. We modeled how soil thickness varies with time, following Dietrich et al. (1986) (Fig. 2a and b). The vertical soil thickness along a hollow axis (Fig. 2b) is a function of diffusivity (K), side slope angle (β), hollow slope angle (θ), and time (t):

$$H_t = \sqrt{2Kt}\left[\left(\tan^2\beta - \tan^2\theta\right)\left(\frac{1}{\cos^2\beta} - \frac{1}{\cos^2\theta}\right)\right]^{1/4} \tag{8}$$

To integrate the soil thickness with the SOC mass balance model (Eq. (3)), the depth of plant C inputs and the decomposition rate (z in Eq. (3)) must be adjusted as deposition occurs. Since the soil production rate is low under thick soils (Eq. (6)), as indicated by cosmogenic isotope data (Heimsath et al., 1997), it is reasonable to assume that the distance of a given soil layer to the soil–bedrock interface (Θ) is a constant in thick depositional soils (Fig. 2b). The depth of a given layer (z) relative to the surface in Eq. (3) is continuously adjusted as:

$$z = H_t - \Theta \tag{9}$$

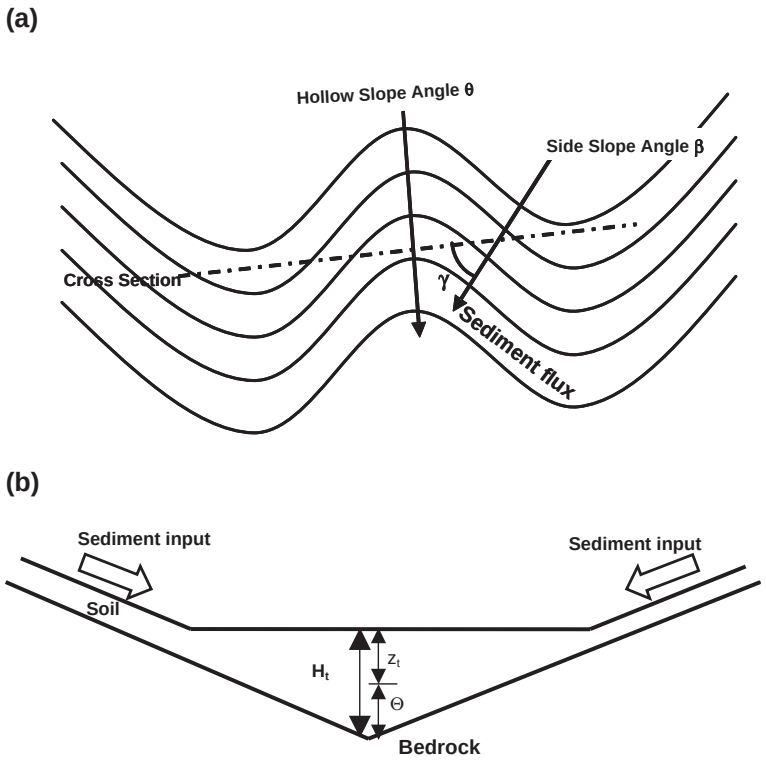

Fig. 2. The geometry of hollows at Tennessee Valley: (a) plan view and (b) simplified cross sectional view used for modeling soil thickness during sediment infilling. Symbols: β is side slope angle, θ is hollow slope angle, H is soil thickness, z is depth from ground surface to soil layer of interest, and Θ is the distance from the soil layer of interest to bedrock.

where z=the soil depth from the land surface [L], and Θ is the distance of that soil layer to the bedrock.

3. Methods

3.1. Study area

The primary study site was Tennessee Valley (TV) in Marin County, CA, U.S.A., and the secondary site was Black Diamond Regional Preserve (BD), Contra Costa County, CA ~50 km east of TV. The areas are characterized by hilly landscapes with average slopes of 30% (TV) and 25% (BD). Past geomorphic research has empirically determined the parameters for the soil transport and production models at both sites (Table 1) (Fernandes and Dietrich, 1997; Heimsath et al., 1997; McKean et al., 1993). At both sites, soil erosion by overland flow was found to be negligible (McKean, 1993; Prosser and Dietrich, 1995; Prosser et al., 1995).

The climate at TV is Mediterranean, with a mean annual precipitation (MAP) of 1200 mm and a mean annual temperature (MAT) of 14 °C (nearby Kensfield weather station). Annual and perennial grasses are mixed with varying densities of coastal shrub. Grazing occurred until 1972 (Dietrich et al., 1995).

Table 1
Site specific model parameters used in the soil erosion and production models

Parameter	Tennessee Valley	Black Diamond
K	50 cm^2 year^{-1}	360 cm^2 year^{-1}
ϕ_o	77±9 m My^{-1}	~1255 m My^{-1}
α	0.23±0.003 m	~0.27 m
ρ_r/ρ_s	2	2
Reference	Heimsath et al. (1997)	K from McKean et al. (1993) P_o and α are calculated from McKean et al. (1993)

The BD site shares the same Mediterranean climate, but is drier and warmer (MAP= 330 mm, MAT= 16 °C) (nearby Antioch Pump Plant 3 weather station). At BD, annual grasses are dominant, and grazing is currently limited to winter months.

The two sites differ greatly in geology, the rates and mechanisms of sediment transport and production, and soils. The TV area is underlain by greywacke sandstone, while the bedrock of BD area is clay-rich marine shale. At TV, soil production and transport occur primarily by pocket gopher burrowing (Black and Montgomery, 1991; Heimsath et al., 1997). This bioturbation produces weakly developed soils with well mixed dark A horizons overlying saprolite. The soils have loam texture. We classified the soils as Lithic Haplustolls to Lithic Ustorthents on convex slopes, and Oxyaquic Haplustolls in hollows. In contrast, at BD, the high clay soils appear to deter gopher colonization, and the seasonal soil shrinking and swelling result in soil creep (McKean et al., 1993) and poorly developed soils with A horizons overlying bedrock. The clay contents of the soils are over 50%. Given the excessive shrinking and swelling of the soils, the clay minerals are largely smectite. The frequency of soil cracks rapidly increases in the downslope direction, as soil thickness increases. We classified the soils on summit as Typic Haploxerolls and soils on shoulders to footslopes as Typic Haploxererts.

3.2. Soil and plant sampling, preparation, and measurements

At both sites, sampling was focused on zero order watersheds with an area of <1 ha. To account for the higher soil variability on convex slopes (due to a range of curvatures), more soil pits were excavated there than on the depositional areas (Fig. 3a and b). At TV, 32 soil pits were excavated on the convex hillslope positions. Additionally, 5 pits were excavated along the axis and boundary of the hollow. For determining soil thickness vs. curvature relationships,

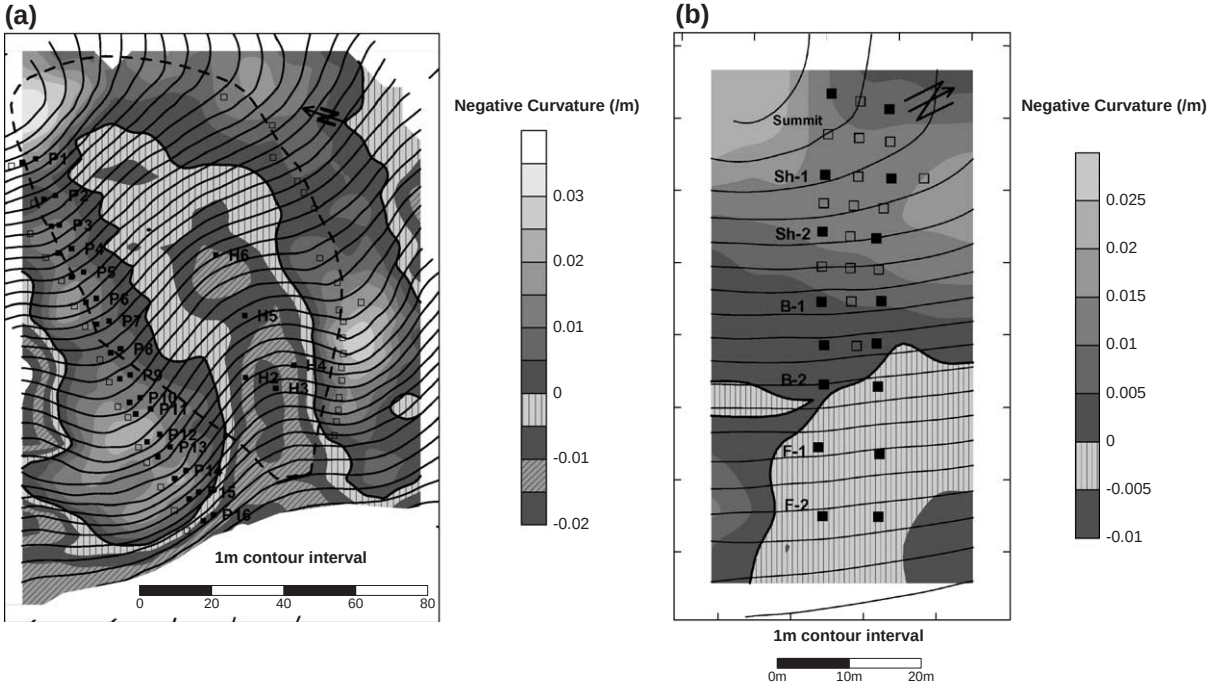

Fig. 3. Topographic maps of study sites: (a) Tennessee Valley and (b) Black Diamond. The filled squares represent soil pits where samples were taken for laboratory analyses. The open squares represent sites where only soil thickness was measured. The dashed line in (a) defines the boundary of the zero order watershed. At Black Diamond (b), the transition from convex to convergent slopes occurs between the B1 and B2 soil sites.

we also measured soil thicknesses at 35 additional soil pits.

At BD, channels have propagated into all surveyed hollows. To focus strictly on diffusive processes, we choose a hillslope where channelization is absent (Fig. 3b). Soil pits were emplaced to capture the major components of a common hillslope model (Ruhe and Walker, 1968): erosional summit, shoulder, and backslope, and a depositional footslope and toeslope. We excavated two soil pits into each hillslope component, resulting in 16 soil pits for soil sampling and analyses. An additional 15 soil pits were augured for soil thickness determinations.

To ensure that we correctly identified the soil–saprolite contact, we excavated soils to depths 20–30 cm below the boundary. The boundaries were generally easy to identify at both sites. At TV, the soils are underlain by fresh sandstone to highly decomposed yellowish saprolite. At BD, fresh shale was observed under dark A horizon-dominated soils. We defined soil thickness as the vertical distance from the ground surface to the saprolite. Soil samples and bulk density cores were collected down to the bedrock–soil interface. To facilitate the spatial analyses, we sampled soils at predetermined depth intervals. The chosen depth increments increased in thickness with soil depth: 0–5, 5–15, 15–30, 30–50 cm, and every 20 cm interval after 50 cm. For the hollows at TV, where thicker and more varied soil horizons developed, sampling was based on soil horizons rather than depth.

A representative sample of air-dried soil was passed through a 2 mm sieve. Approximately 40 g was used for particle size analysis, ~10 g was used for C and N analysis, and the rest was archived. Prior to C and N analysis, the calcareous BD soils were pretreated with HCl fumigation (Harris et al., 2001) to remove inorganic carbon.

The above-ground net primary productivity (ANPP) was measured by harvesting three replicates (0.25 m×0.25 m quadrat) of standing biomass at the end of the growing season (late May) for 3 years (2001–2003). At BD, we report ANPP only for the year 2003, when grazing did not occur (personal communication with park ranger). Harvested plant tissue was dried and weighed following the removal of biomass from preceding years.

The C and N contents of soil and plant samples were measured using a Carlo Erba CN analyzer. Soil particle size was determined by the hydrometer

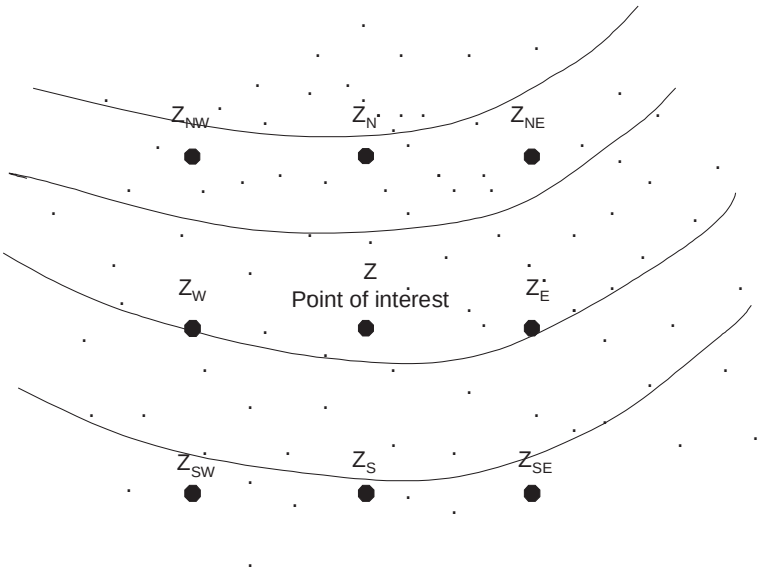

Fig. 4. An illustration of how grid points were used to calculate topographic attributes (Heimsath et al., 1997). Actual cm-accuracy survey points (small dots) were used, using a Kriging method, to generate grid points (filled dots). Contour lines were generated using *Surfer*® software from the grid point data. *Z* is the elevation in meters relative to local reference point.

method (Day, 1965) following pre-treatments with H_2O_2 for organic matter removal and $(NaPO_3)_6$ for clay dispersion. Soil cores of known volume were oven dried at 110 °C and weighed for bulk density. In the case of peds, the volume of a paraffin-coated soil aggregate was determined by displacement in water.

Using these data, the SOC storage for each soil pit was calculated as:

$$S = \sum_{i=1}^{N} \Delta z_i \times \rho_i \times (1 - R_i) \times C_i \quad (10)$$

where S=SOC storage [ML^{-2}], Δz=thickness of sampled horizon [L], ρ=soil bulk density [ML^{-3}], R=mass fraction of >2 mm rock fragments [MM^{-1}], C=mass fraction of carbon [MM^{-1}], subscript i=i-th soil layer, and N=total number of sampled soil layers.

3.3. Surveying and calculation of topographic attributes

Topographic surveys were made with a total laser station (Sokkia CO., LTD) at a 1–2 m interval to calculate curvature. The survey points were gridded using a Kriging method (Surfer software) to create a topographic map. The 4 nearest grid points were used for calculating slope curvature (Fig. 4, adapted from Heimsath et al., 1999) based on the following algorithm in *Surfer*® software.

$$\nabla^2 z = \left(\frac{Z_E - 2Z + Z_W}{\lambda^2}\right) + \left(\frac{Z_N - 2Z + Z_S}{\lambda^2}\right) \quad (11)$$

where Z=elevation [L], and λ=spacing between grids [L]. A 5 m grid size was used because it was the smallest area in which curvature was relatively scale independent.

4. Model parameterization based on field data and observation

One of the key goals of this study is to separate the erosional control on soil thickness from the erosional removal of SOC in terms of their contributions to SOC storage. To address this issue, we first quantify the C erosion and deposition rates, an exercise which requires the parameterization of the C erosion and accumulation model.

4.1. C erosion model on convex slopes

At TV, downslope soil movement occurs when gophers (*Thomomys bottae*) excavate soils onto the ground surface. Burrow collapse also contributes to net downslope sediment transport. To constrain the C content of transported soil, we measured the C content of fresh gopher mounds, which was 2.3±0.1% (n=9). This value closely reflects the C content of the 5–15 cm soil depth, where pocket gophers tend to concentrate their burrowing (Reichman and Seabloom, 2002). The C content of the mound may alternatively reflect a mixture of soil from various depths. In our analyses, 2.3% is used as the C content of eroded soils. The bulk density of eroding soils was estimated to be 1.25 g cm^{-3} (median value of 84 slope bulk density measurements).

At BD, following McKean (1993), we assumed that soil transport velocity [cm $year^{-1}$] decreases from a maximum (V_o) at the soil surface to zero at the soil–bedrock interface (z=H). This agrees with our observation that soil cracking decreases with depth. The sediment flux is the depth integration of the sediment transport velocity profile:

$$\tilde{q}_s = K(-\nabla Z) = \int_0^H V_o\left(1 - \frac{z}{H}\right)dz \quad (12)$$

Since the diffusivity is known (McKean et al., 1993) (Table 1) and the soil thickness and slope gradient were measured, this relationship allows the calculation of the maximum sediment velocity. The averaged C concentration of the eroding soil was estimated by equating the SOC flux ($\rho_\varepsilon C_\varepsilon \tilde{q}_s$) to a depth integration of the SOC velocity profile:

$$\rho_\varepsilon C_\varepsilon K(-\nabla Z) = \int_0^H \rho C_z V_o\left(1 - \frac{z}{H}\right)dz \quad (13)$$

The measured soil bulk density and C concentration profile allowed an estimation of the C concentration (C_ε) of the eroded sediment. An averaged bulk density of 1.36 g cm^{-3} (N=24) was used for the eroding soil. The calculated C concentration of sediment decreases from 2% at the summit to 0.7% on the footslope due to the decreasing C % in the downslope direction.

4.2. Soil C accumulation model at Tennessee Valley

To address the contribution of depositional C inputs to the total SOC in hollows, we simulated the evolution of hollow SOC storage with and without plant C inputs. We first determined the hollow thickness during the infilling process. It is assumed that the hollow had been entirely evacuated at some time=0. This is partially supported by the absence of buried A horizons or irregular C contents or texture with depth. Additionally, all the hollow soils had weakly developed profiles. The simulation was made for 2 locations: H3 and H6, both along the hollow axis (Fig. 3a) where the hillslope profile curvature is zero (condition for Eq. (8)). From the map survey, the side slope angles were estimated to be 18° (H3) and 16° (H6), and the hollow slope angles were 14.6° for both locations.

Additionally, the values of (1) the depositional SOC input (determined as C erosion loss above), (2) in situ plant C input (I_z), and (3) the decomposition rate (k_z) are required to model SOC storage with time. The average value (179 g C m^{-2} $year^{-1}$) of measured hollow ANPP was used as the C input to the soil surface layer (0–5 cm). Root C inputs were considered to decrease exponentially with soil depth ($I=I_o e^{-(z+\Delta z/2)/\eta}$ where I_o=ANPP=179 g C m^{-2} $year^{-1}$), a trend supported by the observed root distributions. We used 10 cm for the e-folding depth of root C inputs because root densities rapidly decreased between 5 and 15 cm depths. A depth interval (Δz) of 5 cm was used. The simulated root C input is approximately twice larger than the above-ground plant C input, a ratio slightly higher than the values (1.1–1.7) reported in Central California annual grassland (Baisden et al., 2002a) but lower than the global estimate for temperate grasslands (3.7) (Jackson et al., 1996).

The decomposition rates of both plant inputs and deposited C were assumed to decrease exponentially with soil depth ($k=k_o e^{-z/v}$). Anoxic conditions that likely occur during winter rainfall (as evidenced by the grey-color of deep soil layers) suggest a decreasing decomposition rate with depth. To determine the decomposition rate at the surface, k_0, a first order decay model with a steady state assumption was used: $dC/dt=I-k_oC=0$, where C is the C content of 0–5 cm soil (2.0±0.2 kg C m^{-2}) and I is the measured above ground plant C input to the hollow (179±5.8 g C m^{-2} $year^{-1}$). The resulting k_o was 0.09±0.01 $year^{-1}$. An e-folding depth (v) of 13 cm was chosen to fit the measured C profile.

Bulk densities were 1.3±0.05 g cm^{-3} (n=16) and 1.7±0.04 g cm^{-3} (n=12) for the upper 50 cm and greater depths, respectively, and the soil thickening rate was adjusted to bulk density changes during the sedimentation. The SOC storage (Eq. (3)) and soil thickness models (Eqs. (8) and (9)) were run at 5 year intervals.

5. Results and discussion

5.1. Observed patterns in soil organic carbon

At both sites, SOC storage varies systematically with slope curvature (Fig. 5), but the SOC storage shows no significant relationships with slope gradient or elevation. More SOC is stored on concave slopes. On convex slopes, the SOC storage decreases with increasing convexity. Likewise, the SOC storage increases with increasing concavity on convergent slopes. In comparing the two sites, the TV hillslope had a wider range of both SOC storage and slope curvatures, though for the same curvature, BD soils had more SOC storage than TV.

In contrast to SOC storage, the soil C % shows little correlation with curvature (Fig. 6). At TV, for a

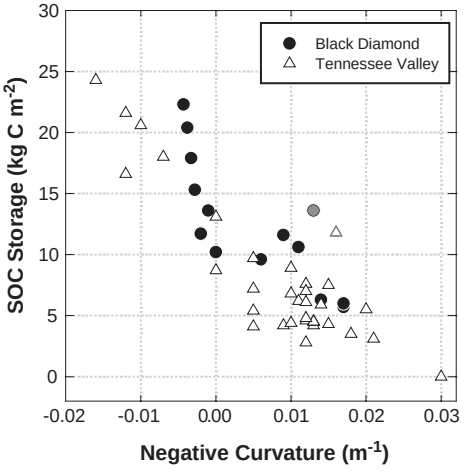

Fig. 5. SOC storage versus negative curvature at Tennessee Valley and Black Diamond. Presumed outliers are identified with a grey color.

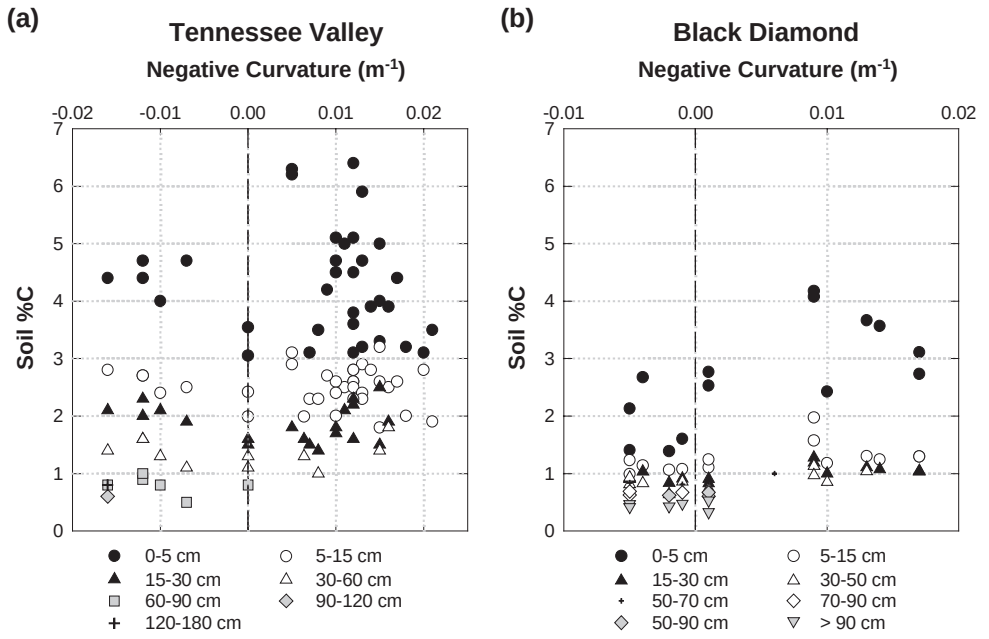

Fig. 6. The measured soil C % at equivalent soil depths vs. slope curvature: (a) Tennessee Valley and (b) Black Diamond.

given depth, soil C % differs little between concave and convex slope positions (Fig. 6a). At BD, the soil C % at a given depth is lower on convergent slopes (Fig. 6b). In comparing the two sites, soil C % is consistently higher at TV, in contrast to the higher SOC storage that occurs at BD.

The patterns of SOC storage and soil C concentration are decoupled at both sites, suggesting that different mechanisms control them. In particular, these patterns emphasize that the strong connection between SOC storage and slope curvature is unrelated to soil C concentrations.

5.2. Biological C cycling and soil carbon concentrations

On convex slopes at TV, spatial variations in soil C % are largely limited to the upper 15 cm. In this shallow soil depth, soil C % and clay content are positively correlated (r=0.86 for 0–5 cm depth, and 0.68 for 5–15 cm depth) and both parameters consistently decrease in a downslope direction, while ANPP shows little spatial trend (Fig. 7a, b, and c). Additionally, the soil surface C % is significantly and positively connected with the C/N ratio (p<0.01, Fig. 8). Lastly, the soil C % in the hollow is similar to that on convex slopes at comparable depths (Fig. 6a).

These results indicate that biological C cycling, rather than soil erosion, dictates spatial variations in soil C %. Spatial variations in decomposition rates, constrained by clay content, appear to affect soil C % more strongly than plant C inputs. In addition, since the ANPP differs little between convex and concave areas (Fig. 9), the similarities in C % indicate that surface decomposition rates in the hollow are similar to those on the convex slopes.

At BD, both the soil surface C % and ANPP decrease in a downslope direction (Fig. 7d and e). While this trend suggests that plant C inputs have an impact on soil C, decomposition rates are also important. The density of soil cracks due to shrinking/swelling increased in the downslope direction (Fig. 7f) because cracks develop only when soil achieves a minimum thickness (Mermut et al., 1996). We hypothesize that increased soil cracking negatively affects the plant productivity and accelerates decomposition, both contributing to reductions in C %.

The differing decomposition rates appear to be the primary cause of the higher soil C % at TV compared to BD. Since the measured ANPP significantly

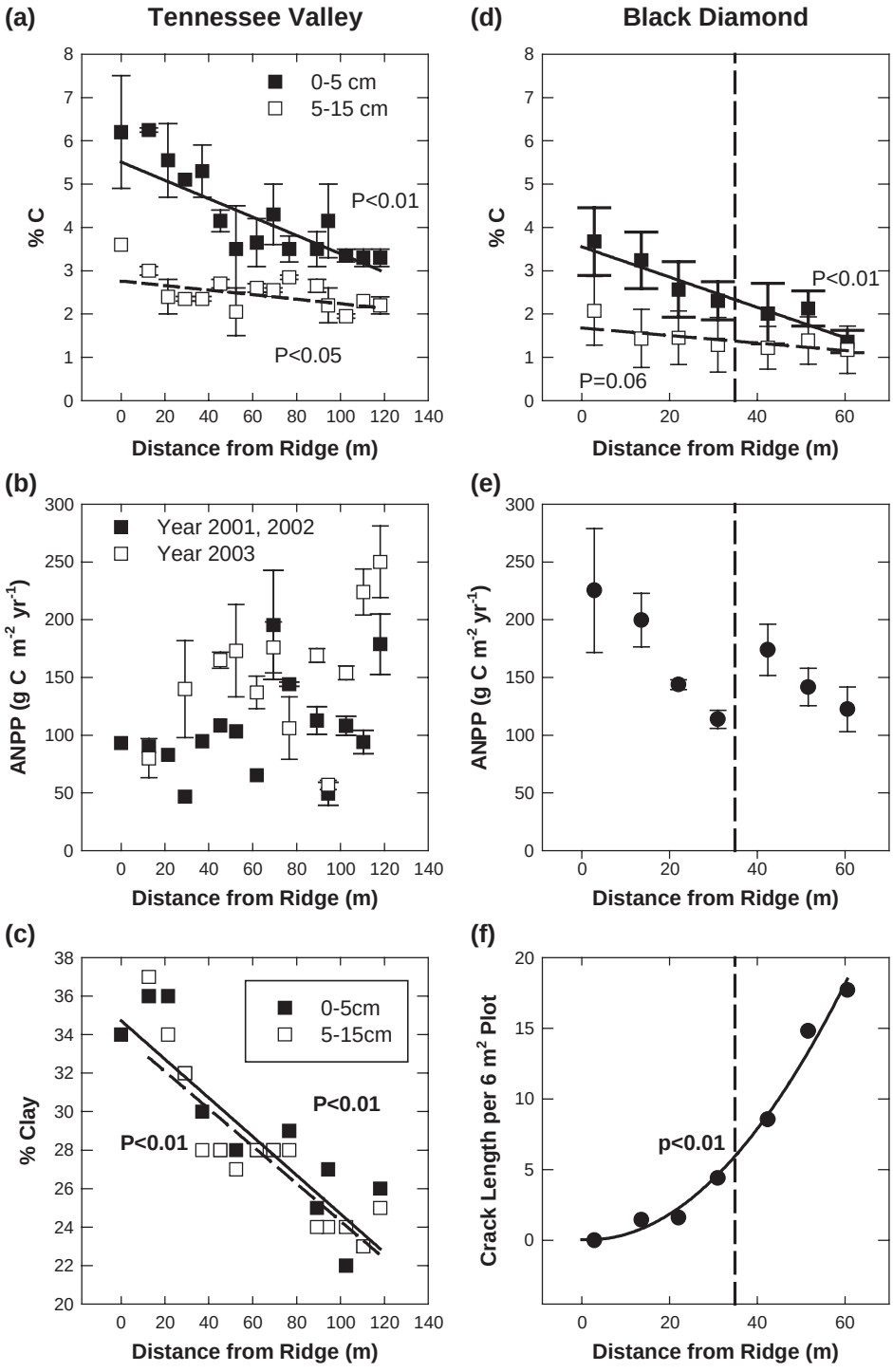

Fig. 7. The variation in soil properties versus slope position at Tennessee Valley [(a) C %, (b) ANPP, and (c) % clay] and at Black Diamond [(d) C %, (e) ANPP, and (f) measured length of visible surface cracks per 6 m^2 plots]. For the Black Diamond figures, the left side of the vertical dashed line represents convex slopes, and the right side represents concave slopes. The error bars indicate standard errors.

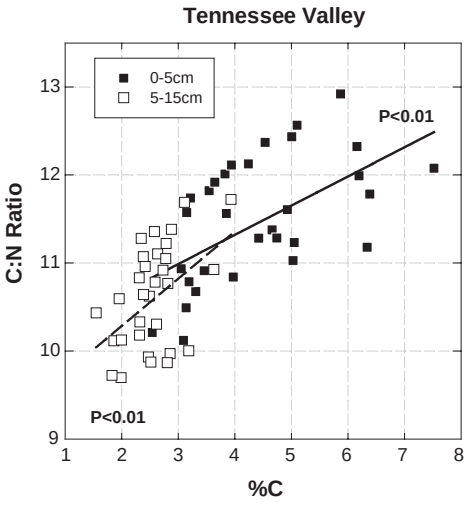

Fig. 8. The relationship between the C % and the C/N ratio of soil surface layers at Tennessee Valley.

overlaps between the two sites (60 to 250 g C m^{-2} $year^{-1}$ at TV and from 110 to 220 g C m^{-2} $year^{-1}$ at BD in year 2003, Fig. 7b and e), it is likely that higher decomposition rates due to warmer and drier conditions result in the lower soil C % at BD.

The insensitivity of soil C % to curvature at both sites suggests that biological C cycling is far faster than erosion rates. To examine this, sediment transport can be viewed in terms of residence times: the average time an individual soil particle remains within a soil volume. Residence time is inversely related to the rate of soil transport, and thus slope gradient. The soil C % on convex slopes does not correlate with the inverse of slope (data not shown), and the rates of biological C cycling therefore must greatly exceed that of physical soil transport.

5.3. SOC storage and soil thickness versus C erosion: convex slopes

The analyses indicate that the surface soil C % is controlled by biological C fluxes independently of curvature, but SOC storage is curvature-dependent. Curvature controls the rate of soil erosion, and soil erosion affects SOC storage through two different pathways. First, soil erosion, together with the C content of eroding soil, determines the rate of C erosion losses. Second, soil erosion, combined with soil production, determines the soil thickness and thus the soil's capacity to store C.

First, we investigate whether erosional losses of C cause the curvature-dependent SOC storage. Although SOC storage is negatively correlated with C erosion rates (Fig. 10), this correlation does not imply a causal relationship. The possible range in

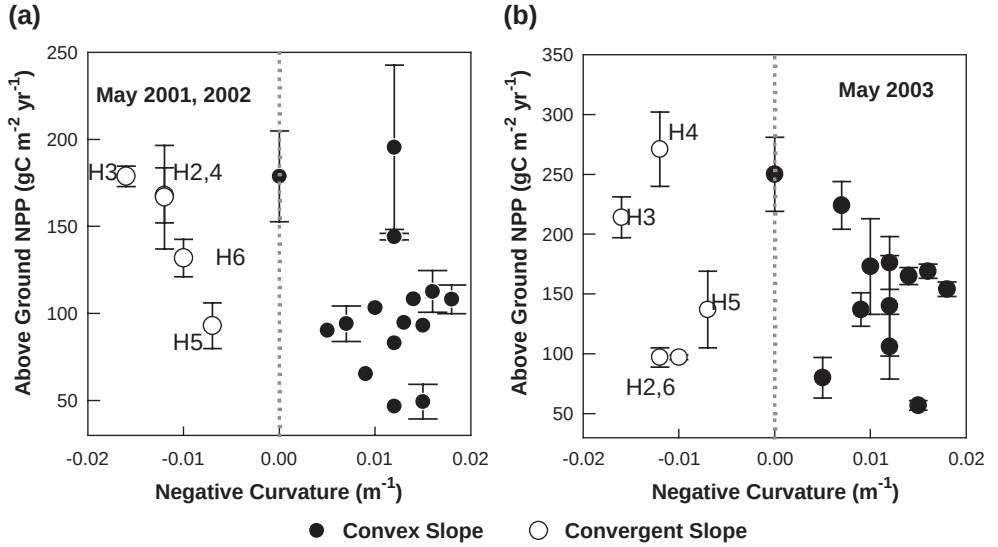

Fig. 9. The measured ANPP versus slope curvature at Tennessee Valley in (a) 2001 and 2002 and (b) 2003.

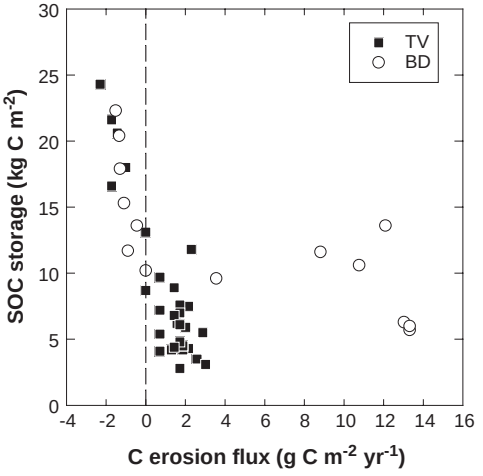

Fig. 10. The relationship between calculated C erosion rates and soil C storage for the two study sites.

SOC storage created solely by C erosion rates was calculated using Eq. (2). In this model, the steady state SOC storage is $(I-\rho_\varepsilon C_\varepsilon E)/k$ and I/k for eroding and non-eroding areas, respectively. The ratio, $(1-\rho_\varepsilon C_\varepsilon E/I)$, is therefore directly related to the rates of C erosion and plant C input. We incorporated the range of the calculated C erosion losses and the measured ANPP into this ratio. The maximum C erosion reduced the SOC storage by only 3% relative to non-eroding sites at TV, and 8% at BD. Since this is only a small fraction of the observed range of SOC storage (0 to 13.1 kg C m^{-2} at TV and 5.7 to 13.6 kg C m^{-2} at BD), it appears that C erosion contributes little to the curvature-dependent SOC storage patterns for these two locations.

Based on the full soil C mass balance model (Eqs. (3) and (4)), it now seems appropriate that erosion is most responsible for the observed SOC storage pattern by creating the curvature-dependent soil thickness distribution. The values of SOC storage and soil thickness are tightly related at both sites (Fig. 11), and the spatial pattern of soil thickness largely agrees with the modeled steady state soil thicknesses based on empirically constrained soil erosion and production functions (Eq. (7), Fig. 12b and c).

In spite of this relationship between SOC storage and soil thickness (Fig. 11), it is difficult to empirically prove the effect of erosion on SOC storage through soil thickness because of the slow rate of soil thickness change (and the assumption that soils are at steady state). Instead, we examine the relationship by considering a case where the soil erosion rate doubles from 0.06 mm $year^{-1}$ to 0.12 mm $year^{-1}$, both of which are within the range of erosion rates at TV. The doubled erosion rate reduces soil thickness from ~40 cm to ~10 cm within 10^4 years (Eq. (8)). At TV, a 10 cm thick soil (2.0 kg C m^{-2}) stores 27% of the SOC stored in 40 cm thick soils (7.5 kg C m^{-2}) (Fig. 11). On the other hand, this change in erosion rate doubles the C erosion rate only from 1.95 g C m^{-2} $year^{-1}$ to 3.9 g C m^{-2} $year^{-1}$, a change which we showed earlier is incapable of significantly affecting SOC storage Thus, erosion is apparently responsible for the observed SOC storage pattern through its effect on the curvature-dependent soil thickness distribution rather than by its direct removal of soil C.

In a comparison of the two sites, BD has the highest SOC storage at a given curvature (Fig. 5), despite a lower soil C %. This is due to thicker soils at BD for a given curvature (Fig. 12a). While the soil erosion loss at BD is 7 times greater (at the same curvature) than at TV, this is compensated for by even

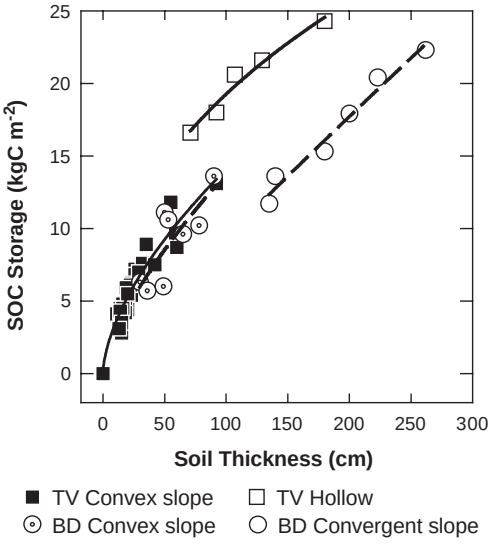

Fig. 11. The relationships between soil thickness and soil organic C storage for different slope segments of the study sites. [TV convex slope: $y=(0.8553\pm0.1099)x^{(0.6084\pm0.0387)}$, $r^2=0.90$; TV hollow: $y=(2.872\pm0.15824)x^{(0.413\pm0.0423)}$, $r^2=0.96$; BD convex slope: $y=(0.565\pm0.5005)x^{(0.6932\pm0.2139)}$, $r^2=0.60$; BD footslope: $y=(0.137\pm0.0625)x^{(0.918\pm0.0855)}$, $r^2=0.96$).]

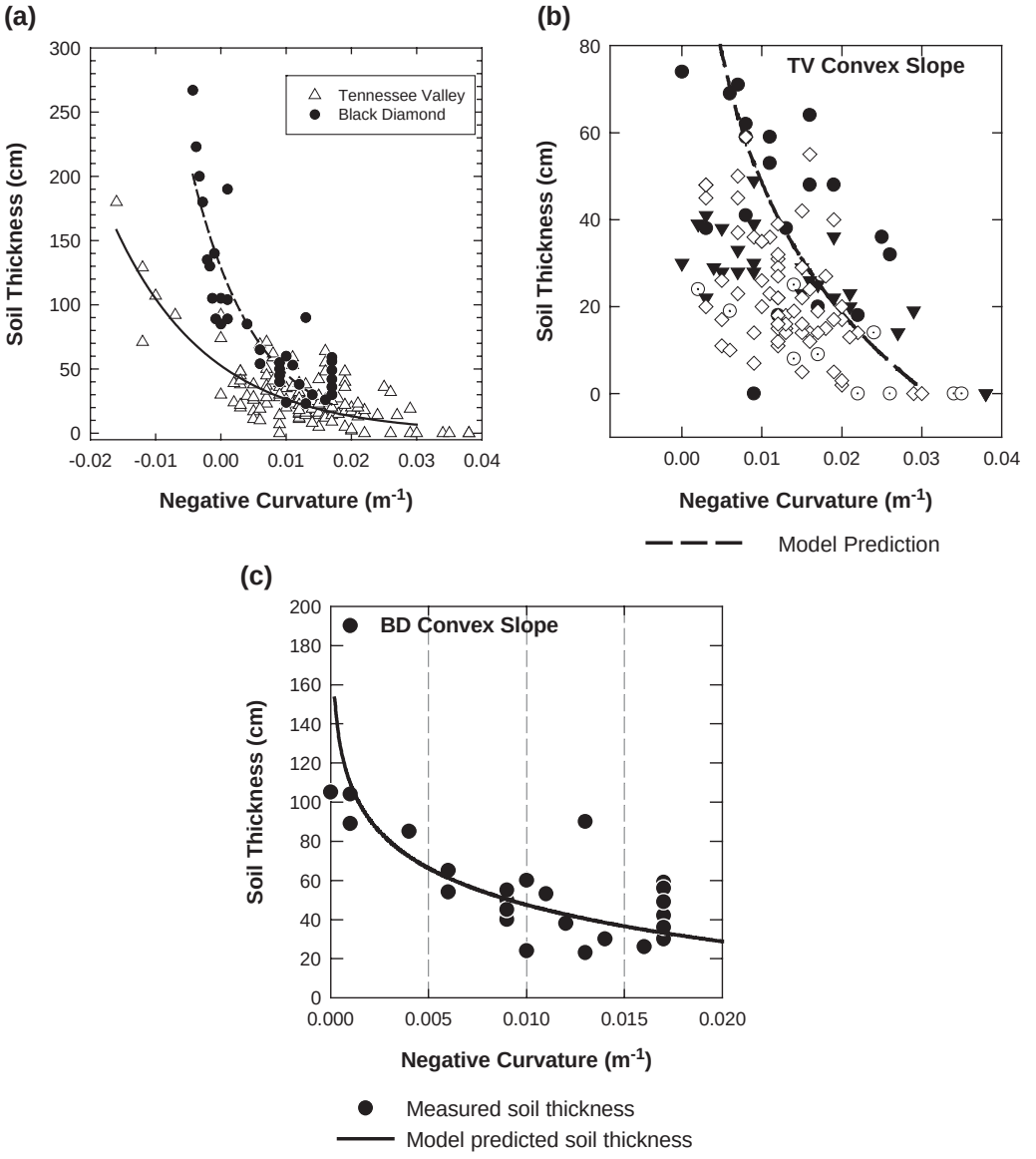

Fig. 12. The relationships between slope curvature and soil thickness for: (a) entire watershed (Tennessee Valley: y=(51.434±2.3732)$e^{(-69.612\pm3.8061)x}$, r^2=0.78; Black Diamond: y=(101.094±4.246)$e^{(-200.110\pm13.1030)x}$, r^2=0.92), (b) TV convex slope, and (c) BD convex slope. The symbols in (b) represent individual hillslopes including our data (empty diamonds) and data from Heimsath et al. (1997).

higher production rates of soil from the soft shale bedrock (McKean et al., 1993; Monaghan et al., 1992) (Table 1). Additionally, TV soils are composed of 25±3.3% rock fragments (>2 mm), which further reduces the effective soil volume for C storage, while the rock content in BD soils is nearly zero. Thus, the bedrock-driven differences in soil thickness control the volume for C storage and cause the SOC storage differences between the sites.

Despite the strong relationship between SOC storage and soil thickness, the measured SOC storage often deviates from the fitted relationships (Fig. 11).

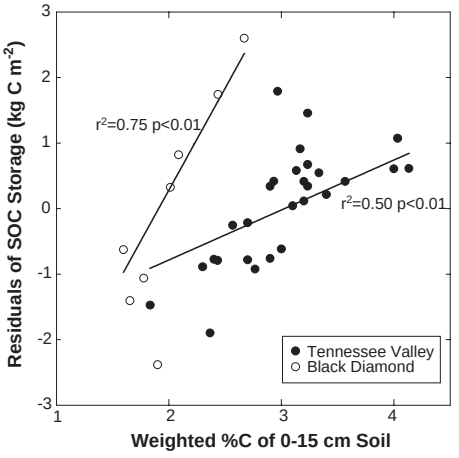

Fig. 13. A linear regression of residuals obtained in the comparison of SOC storage vs. soil thickness plotted against the depth weighted C % of the 0–15 cm soil depth.

The deviations are mostly due to the variations in soil C %. The differences (residuals) between measured SOC storage and values predicted from the fitted relationships were regressed against the weighted C % of the 0–15 cm soil layer (Fig. 13). The C % explained a significant portion of the residuals: 50% at TV and 75% at BD. Thus, biological C cycling, and its affect on soil C %, contributes to the variations in SOC storage, but the effect is of secondary importance and is not curvature-dependent.

5.4. SOC storage and soil thickness versus C erosion: concave slopes

On concave slopes, SOC storage is positively related with C depositional rates (Fig. 10) and with soil thickness (Fig. 11). To determine the relative importance of these two factors on observed C storage patterns, the fate (turnover time) of deposited C must be known. Based on the hollow soil thickness model (Eq. (8)) at TV, 11–13 ky is required to fill the hollow to its current thickness (Fig. 14a). The simulated SOC storage for site H3 during that time period (Eq. (3)) shows a nonlinear increase over time, ending with amounts close to the measured value of 24.3 kg C m^{-2} (Fig. 14b). However, if this model is run without plant C inputs, the results show that ~56 kg C m^{-2} is deposited by erosion (180 cm thick sediment with 2.3 C %), but nearly all of this is oxidized following deposition. Thus, for reasonable decomposition rates, erosional deposition of C seems to have little impact on hollow soil SOC storage.

Eroded C may have longer turnover times than we used above, which would increase the importance of deposited C in hollow C storage. To evaluate this, we use a value of $0.01 \times \exp(-z/10)$ $year^{-1}$ as the lower end of likely decomposition rates, which represents C turnover times of 100 years at the soil surface and 1000 years at a soil depth of 23 cm. For this lower decomposition rate, only 1.7 kg C m^{-2} of SOC storage

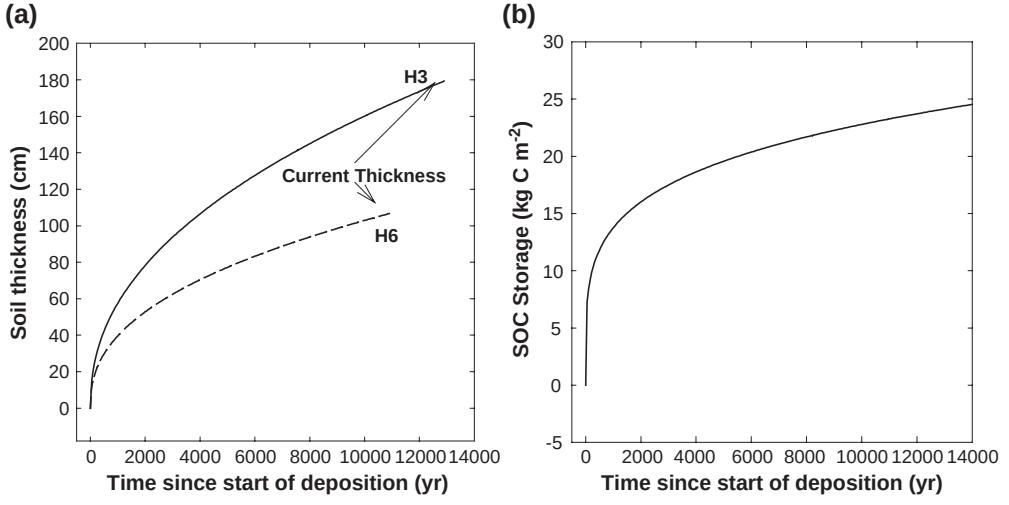

Fig. 14. Calculated trends in (a) hollow soil thicknesses during infilling following a landslide and (b) the SOC storage during the infilling.

would be present after 13 ky if no plant inputs occurred. These low decomposition rates seem unwarranted because eroded soil C should contain a high proportion of labile soil C because it is derived from the eroding soil surface where C turnover times of less than 100 years have been observed for grasslands in central California (Baisden et al., 2002b).

The calculations above show that for reasonable decomposition rates, C deposition cannot explain the high SOC storage in depositional settings at TV. Supporting this interpretation, the C/N ratios in the hollow are consistently higher than soils on convex slopes (data not shown), implying a greater labile C component, presumably from in situ plant inputs. A similar situation likely exists at BD, where the current depositional C input (Fig. 10) is only ~1% of in situ ANPP.

Biological rates of C cycling are fast relative to sedimentation. Thus, the soil surface C % is unrelated to deposition (or erosion) rates. The observed soil C profiles are essentially the same for all of the hollow soils, regardless of their curvatures or deposition rates (Fig. 6a). This is supported by the modeling which indicates that the C profile does not vary across a wide range in sedimentation rates during the hollow infilling (Fig. 15). Therefore, SOC

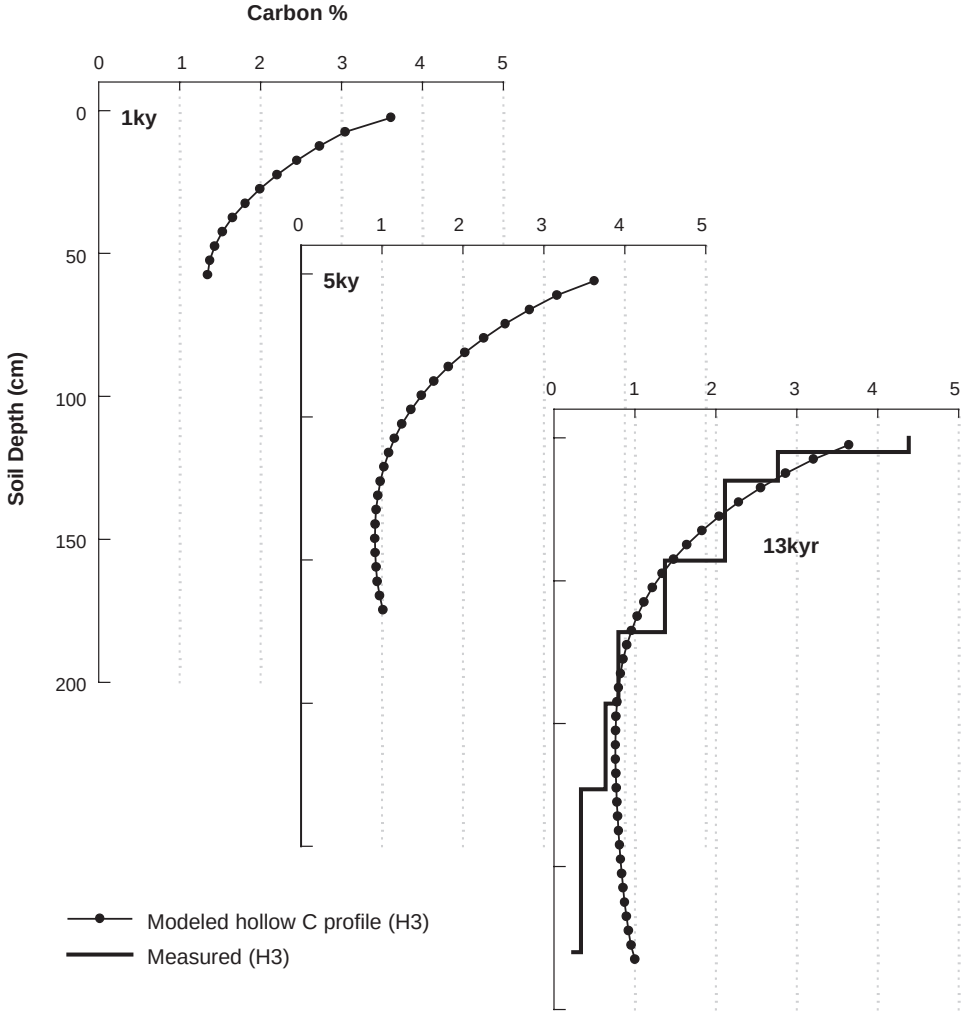

Fig. 15. Simulations of soil C vs. depth in the TV hollow during infilling, with a comparison to measured values assuming hollow is ~13 ka.

storage in hollows (like convex areas) is controlled by soil depth, and the soils contain mainly in situ plant derived C.

Besides soil thickness, several secondary factors alter the volume available for C storage. First, differences in the SOC storage vs. soil thickness relationships exist for convex and concave portions of the landscape (Fig. 11). At TV, this discontinuity is due to a lower rock content in the hollow (9±1.3%) vs. convex soils (25±3.3%). The difference in rock contents between the concave/convex sites thus accounts for the 21% difference in SOC storage per unit volume. At BD, in contrast to TV, the SOC storage (per unit soil thickness) decreases in the footslope (Fig. 11) due to a lower soil C % (Fig. 6).

For the same curvature on concave slopes, the SOC storage is usually greater at BD than at TV (Fig. 5). Soils at BD are significantly thicker than TV due to a 7 fold higher depositional rate (Fig. 12a). Thus, at a given curvature, the thicker soils at BD, despite their generally lower soil C concentrations, store more SOC than soils at TV.

5.5. Soil organic carbon storage within watersheds

The empirical relationships between SOC storage, soil thickness, and curvature, were combined to produce a map of watershed SOC storage (Fig. 16). The differences between the measured SOC storage and the model predicted values were quantified (Fig. 16a and b), revealing only small differences. The hillslopes were divided into convex and convergent areas based on the curvature, and their surface areas and stored SOC were calculated using *Surfer*® software. The results of the calculations are summarized in Table 2.

At TV, the watershed (within the encircled boundary in Fig. 3a) contains 110 t C of SOC in an area of 8023 m^2. The average SOC storage is 14 kg C m^{-2}. The convex slopes, comprising 47% of the total area, contain 29% of the watershed SOC. In contrast, the depositional area contains 71% of the watershed SOC, though it represents 53% of the watershed area.

At BD, the hillslope contains 35 t C of SOC in an area of 2559 m^2. The average SOC storage is also (like TV) 14 kg C m^{-2}. The depositional segments

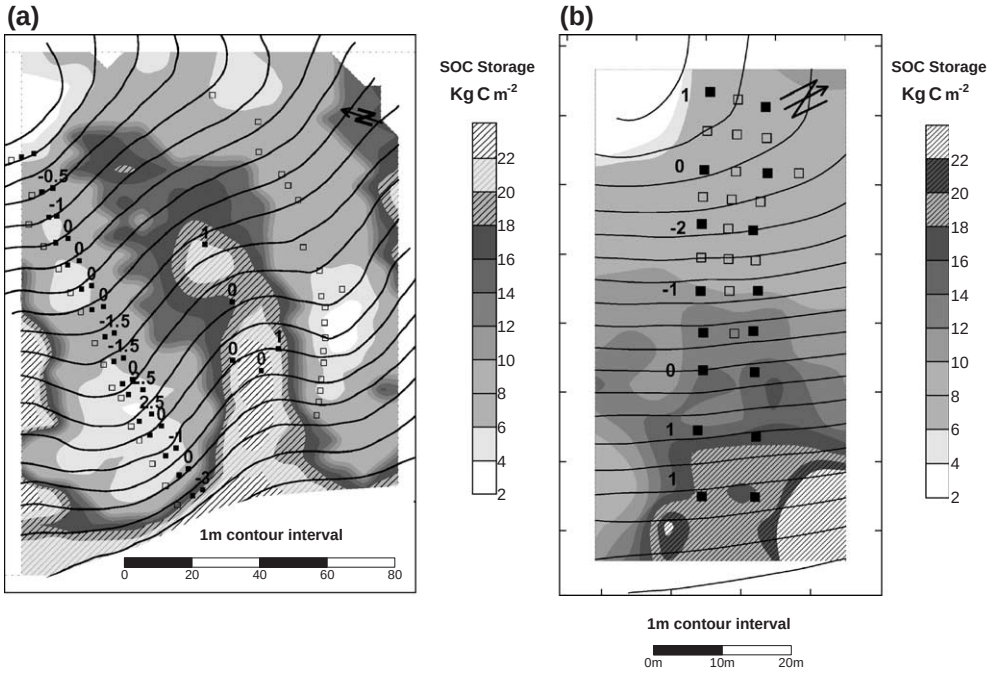

Fig. 16. The calculated SOC storage maps for (a) Tennessee Valley and (b) Black Diamond. The numbers on the figures are model errors larger than 0.5 kg C m^{-2}, and were obtained by subtracting the model estimates from the measured SOC storage at a given position.

Table 2
The spatial distribution of soil organic carbon within the watersheds examined in the study

Site	Parameter	Entire watershed	Convex hillslope	Convergent hollow
Tennessee Valley	stored SOC (tC)	110	32 (29%)	78 (71%)
	surface area (m^2)	8023	3734 (47%)	4289 (53%)
	SOC storage (kg C m^{-2})	14	9	18
Black Diamond	stored SOC (tC)	35	17	18
	surface area (m^2)	2559	1706	853
	SOC storage (kg C m^{-2})	14	10	21

which comprise 33% of the area contain 51% of the hillslope C. However, at BD, the toeslope extends another ~40 m downslope beyond the area shown in Fig. 3b. Assuming that the footslope SOC storage is constant in concave areas (a conservative assumption given the observation that soil thickens rapidly in a downslope direction), the SOC storage averaged over the entire hillslope is 16 kg C m^{-2} at BD. In this case, the depositional slope stores 68% of the total hillslope SOC.

These results indicate that the largest portion of upland SOC is stored in depositional areas that are subject to cyclic evacuation. At TV, the hollows are the focal point of episodic landslides (Reneau and Dietrich, 1987). At BD, shallow to deep bedrock earthflows occur in footslopes to toeslopes (McKean, 1993). Consequently, ~70% of upland hillslope SOC (in our areas) is susceptible to episodic mass wasting events. In contrast, the remaining ~30% of SOC is stored on convex slopes that undergo continuous soil erosion and production.

6. Conclusions

To our knowledge, this is the first study of the spatial distribution of soil C on hillslope using integrated biological C cycling and sediment transport. The C mass balance model we introduce (Eqs. (3) and (4)) provides a quantitative framework to design and interpret studies of soil C on vegetated uplands. The key findings were that while biological C fluxes appear responsible for the spatial variation in the soil surface C concentrations that is largely independent of curvature, there is a strong curvature-dependent SOC storage caused by curvature-dependent soil erosion/production and their integrated effect on soil thickness. By comparing two contrasting sites (geology and climate), we found that the cooler and wetter TV site, despite having the highest soil C %, had a lower SOC storage. This was due to shallower soil thicknesses that resulted from lower soil production and sediment transport rates at TV (sandstone) than at the shale-rich BD site. Thus, as others have emphasized (Jobbagy and Jackson, 2000), it is necessary to sample the entire soil thickness, rather than predetermined depth intervals, in order to accurately assess the spatial variation in SOC within a hillslope and compare the SOC storage of hillslopes in differing environments, which is important for quantifying global SOC storage.

The studied sites may lie at one end of a natural range in the relative importance of sediment transport vs. biological C cycling, and their effects on soil C storage. Regardless of the absolute values of these processes, the model (Eqs. (3) and (4)) can be applied to other areas by using appropriate soil erosion and production models. While conceptually straightforward, parameterizing these models requires time and funding, particularly for cosmogenic nuclide-based estimates of soil production rates. Thus, a fruitful approach should involve multidisciplinary teams and questions, where the focus on soil characteristics is part of a larger geomorphic effort. This effort is needed to fully understand the chemistry of soils along topographic gradients, one of the most fundamental controls on soil and ecosystem properties (Jenny, 1941), and one which has only recently succumbed to mechanistic analyses. Ultimately, the integration of physical and biological processes in our model will lead to a more mechanistic explanation of the topographic variations in C, N, and other elemental cycles in diverse ecosystems of the globe.

Acknowledgements

We thank Aaron Miller, Matt Cover, Cristina Castanha, Jonathan Sanderman, Stephanie Ewing,

Michale Chendorain, Sungjoo Lee, Minkoo Kim, and Jaeyeoun Won for their help in field work. This study was funded by the National Science Foundation, Kearney Foundation of Soil Science, and the Berkeley Academic Senate Committee on Research.

References

Aandahl, A.R., 1948. The characterization of slope positions and their influence on total nitrogen content of a few virgin soils of western Iowa. Proceedings-Soil Science Society of America 13, 449–454.

Amundson, R., 2001. The carbon budget in soils. Annual Review of Earth and Planetary Sciences 29, 535–562.

Baisden, W.T., et al., 2002a. A multiisotope C and N modeling analysis of soil organic matter turnover and transport as a function of soil depth in a California annual grassland soil chronosequence. Global Biogeochemical Cycles 16 (4), 1135.

Baisden, W.T., Amundson, R., Cook, A.C., Brenner, D.L., 2002b. Turnover and storage of C and N in five density fractions from California annual grassland surface soils. Global Biogeochemical Cycles 16 (4) (art. no. 1117).

Black, T.A., Montgomery, D.R., 1991. Sediment transport by burrowing mammals, Marin County, California. Earth Surface Processes and Landforms 16, 163–172.

Brejda, J.J., et al., 2001. Estimating surface soil organic carbon content at a regional scale using the national resource inventory. Soil Science Society of America Journal 65, 842–849.

Burke, I.C., et al., 1999. Spatial variability of soil properties in the shortgrass steppe: the relative importance of topography, grazing, microsite, and plant species in controlling spatial patterns. Ecosystems 2, 422–438.

Culling, W.E.H., 1963. Soil creep and the development of hillside slopes. The Journal of Geology 71 (2), 127–161.

Day, P.R., 1965. Particle fractionation and particle-size analysis. In: Black, C.A. (Ed.), Methods of Soil Analysis, vol. 1. American Society of Agronomy, pp. 545–567.

Dietrich, W.E., Wilson, C.J., Reneau, S.L., 1986. Hollows, colluvium, and landslides in soil-mantled landscapes. In: Abrahams, A.D. (Ed.), Hillslope Processes, Sixteenth Annual Binghamton Symposia in Geomorphology. Allen and Unwin, Boston, pp. 361–388.

Dietrich, W.E., Reiss, R., Hsu, M.L., Montgomery, D.R., 1995. A process-based model for colluvial soil depth and shallow landsliding using digital elevation data. Hydrological Processes 9 (3–4), 383–400.

Fernandes, N.F., Dietrich, W.E., 1997. Hillslope evolution by diffusive processes: the timescale for equilibrium adjustments. Water Resources Research 33 (6), 1307–1318.

Garten, C.T., Ashwood, T.L., 2002. Landscape level differences in soil carbon and nitrogen: implications for soil carbon sequestration. Global Biogeochemical Cycles 16 (4), 61:1–61:14.

Gessler, P.E., Chadwick, O.A., Chamran, F., Althouse, L., Holmes, K., 2000. Modeling soil–landscape and ecosystem properties using terrain attributes. Soil Science Society of America Journal 64 (6), 2046–2056.

Gilbert, G.K., 1909. The convexity of hilltops. Journal of Geology 17, 344–350.

Harris, D., Horwáth, W.R., Kessel, C.V., 2001. Acid fumigation of soils to remove carbonates prior to total organic carbon or carbon-13 isotopic analysis. Soil Science Society of America 65, 1853–1856.

Heimsath, A.M., Dietrich, W.E., Nishiizumi, K., Finkel, R.C., 1997. The soil production function and landscape equilibrium. Nature 388, 358–361 (July 24).

Heimsath, A.M., Dietrich, W.E., Nishiizumi, K., Finkel, R.C., 1999. Cosmogenic nuclides, topography, and the spatial variation of soil depth. Geomorphology 27, 151–172.

Heimsath, A.M., Chappell, J., Dietrich, W.E., Nishiizumi, Kunihiko, Finkel, R.C., 2000. Soil production on a retreating escarpment in southeastern Australia. Geology 28 (9), 787–790.

Heimsath, A.M., Chappell, J., Dietrich, W.E., Nishiizumi, K., Finkel, R.C., 2001a. Late Quaternary erosion in southeastern Australia: a field example using cosmogenic nuclides. Quaternary International 83–85, 169–185.

Heimsath, A.M., Dietrich, W.E., Nishiizumi, K., Finkel, R.C., 2001b. Stochastic processes of soil production and transport: erosion rates, topographic variation, and cosmogenic nuclides in the Oregon Coast Range. Earth Surface Processes and Landforms 26, 531–552.

Honeycutt, C.W., Heil, R.D., Cole, C.V., 1990. Climatic and topographic relations of three great plains soils: II. Carbon, nitrogen, and phosphorus. Soil Science Society of America Journal 54, 476–483.

Hook, P.B., Burke, I.C., 2000. Biogeochemistry in a shortgrass landscape: control by topography, soil texture, and microclimate. Ecology 81 (10), 2686–2703.

Jackson, R.B., et al., 1996. A global analysis of root distributions for terrestrial biomes. Oecologia 108, 389–411.

Jenny, H., 1928. Relation of climatic factors to the amount of nitrogen in soils. Journal-American Society of Agronomy 20, 900–912.

Jenny, H., 1941. The Factors of Soil Formation. McGraw-Hill, New York.

Jobbagy, E.G., Jackson, R.B., 2000. The vertical distribution of soil organic carbon and its relation to climate and vegetation. Ecological Applications 10 (2), 423–436.

Kleiss, H.J., 1970. Hillslope sedimentation and soil formation in northeastern Iowa. Proceedings-Soil Science Society of America 34, 287–290.

McKean, J.A., 1993. Soil Creep and Earthflows. University of California at Berkeley, Berkeley. 363 pp.

McKean, J.A., Dietrich, W.E., Finkel, R.C., Southon, J.R., Caffee, M.W., 1993. Quantification of soil production and downslope creep rates from cosmogenic 10Be accumulations on a hillslope profile. Geology 21, 343–346 (April).

Mermut, A.R., Dasog, G.S., Dowuona, G.N., 1996. Soil morphology. In: Ahmand, A., Mermut, A. (Eds.), Vertisols and Technologies for their Management. Elsevier, Amesterdam, pp. 89–114.

Minasny, B., McBratney, A.B., 1999. A rudimentary mechanistic model for soil production and landscape development. Geoderma 90, 3021.

Minasny, B., McBratney, A.B., 2001. A rudimentary mechanistic model for soil formation and landscape development: II. A two-dimensional model incorporating chemical weathering. Geoderma 103, 161–179.

Monaghan, M.C., McKean, J., Dietrich, W., Klein, J., 1992. ^{10}Be chronometry of bedrock-to-soil conversion rates. Earth and Planetary Science Letters 111, 483–492.

Moore, I.D., Gessler, P.E., Nielsen, G.A., Peterson, G.A., 1993. Soil attribute prediction using terrain analysis. Soil Science Society of America Journal 57, 443–452.

Park, S.J., McSweeney, K., Lowery, B., 2001. Identification of the spatial distribution of soils using a process-based terrain characterization. Geoderma 103, 249–272.

Post, W.M., Emanuel, W.R., Zinke, P.J., Stangenberger, A.G., 1982. Soil carbon pools and world life zones. Nature 298, 156–159 (8 July).

Prosser, I.P., Dietrich, W.E., 1995. Field experiments on erosion by overland flow and their implication for a digital terrain model of channel initiation. Water Resources Research 31 (11), 2867–2876.

Prosser, I.P., Dietrich, W.E., Stevenson, J., 1995. Flow resistance and sediment transport by concentrated overland flow in a grassland valley. Geomorphology 13 (1–4), 71–86.

Reichman, O., Seabloom, E.W., 2002. The role of pocket gophers as subterranean ecosystem engineers. Trends in Ecology and Evolution 17, 44–49.

Reneau, S.L., Dietrich, W.E., 1987. The importance of hollows in debris flow studies; examples from Marin County, California. Geological Society of America. Reviews in Engineering Geology 7, 165–179.

Rosenbloom, N.A., Doney, S.C., Schimel, D.S., 2001. Geomorphic evolution of soil texture and organic matter in eroding landscapes. Global Biogeochemical Cycles 15 (2), 365–381.

Ruhe, R.V., Walker, P.H., 1968. Hillslope models and soil formation: I. Open systems. Transactions of the 9th International Congress on Soil Science 6 (4), 551–560.

Sanderman, J., Amundson, R.G., Baldocchi, D.D., 2003. Application of eddy covariance measurements to the temperature dependence of soil organic matter mean residence time. Global Biogeochemical Cycles 17 (2) (Art. No. 1061).

Schimel, D., Stillwell, M.A., Woodmansee, R.G., 1985. Biogeochemistry of C, N, and P in a soil catena of the shortgrass steppe. Ecology 66 (1), 276–282.

Stallard, R.F., 1998. Terrestrial sedimentation and the carbon cycle: coupling weathering and erosion to carbon burial. Global Biogeochemical Cycles 12 (2), 231–257 (June).

Trumbore, S., Chadwick, O.A., Amundson, R., 1996. Rapid exchange between soil carbon and atmospheric carbon dioxide driven by temperature change. Science 272, 393–396 (April 19).

Yonker, C.M., Schimel, D.S., Paroussis, E., Heil, R.D., 1988. Patterns of organic carbon accumulation in a semiarid shortgrass steppe, Colorado. Soil Science Society of America Journal 52, 478–483.

Yoo, K., Amundson, R., Heimsath, A.M., Dietrich, W.E., in press. Erosion of upland hillslope soil organic carbon: coupling field measurements with a sediment transport model. Global Biogeochemical Cycles.

Young, F., Hammer, R., 2000. Soil–landscape relationships on a loess-mantled upland landscape in Missouri. Soil Science Society of America Journal 64 (4), 1443–1454.